AIAA 81-4092

Thermal Stress Analysis of Layered Cylindrical Shells

Craig J. Miller*
Case Western Reserve University, Cleveland, Ohio
William A. Millavec†
TRW Corporation, Redondo Beach, Calif.
and
Thomas P. Kicher‡
Case Western Reserve University, Cleveland, Ohio

The use of layered metal-ceramic composite panels as abradable tip seals in jet engines may lead to significant increases in engine efficiency. This paper describes the development of a thermal stress analysis capability based on classical shell theory for the analysis of panels with all four edges free. Various boundary conditions on the top and bottom surfaces of the plate are examined. The material properties can be isotropic, transversely isotropic, or orthotropic, and may be functions of temperature. All heat flow takes place in the radial direction, allowing a one-dimensional heat transfer analysis. Solutions for the case of top and bottom surfaces fully restrained, top and bottom surfaces free to move tangentially but not radially, and for the case of a flat plate completely unrestrained can be obtained in closed form directly from the force-strain relations. Examples of solutions for each of these types of boundary conditions are presented. The solution for a curved plate cooled with no external restraints cannot be obtained directly from the force-strain relations. For that case, a Rayleigh-Ritz analysis was used. Assumed displacement functions are chosen for u, v, and w, with unknown participation parameters. Using the force equilibrium equations, the unknown parameters in u and v can be expressed in terms of the parameters of w. The potential energy is then minimized with respect to the parameters of w to find the equilibrium state. The analysis capability was then used to explain the fractures and deformations resulting from fabrication and anticipated use. The analysis can also be used to develop alternate fabrication strategies to maximize the production yield.

Introduction

THE use of layered metal-ceramic composite panels as abradable tip seals in jet engines may lead to significant increases in engine efficiency. As indicated in Fig. 1, the seal consists of a number of cylindrical shell segments mounted on a relatively rigid track to form a ring. As the engine is fired, the turbine blades lengthen due to the combined effect of centrifugal force and temperature increase. The composite is abraded and a very effective seal is formed.

During the fabrication process, layers of ceramic are deposited onto a metallic surface and fused into a single structural element. The process involves the application of heat and pressure to achieve a consistent structural integrity. When the segments are removed from the press and examined at room temperature, a variety of cracks have been observed. Occasionally delamination cracks have been observed between the internal ceramic layers. On other occasions, radial cracks can be observed within a single ceramic layer. Direct experimental techniques to measure the stresses were judged to be impossible. Since the bulk properties of the constituent materials were known, a structural analysis of the cure process was attempted to provide an insight into the source of these deleterious stresses.

The purpose of this study was to develop an analytical model for predicting the stresses in a layered metal-ceramic composite. The results of the analysis must qualitatively predict stresses consistent with the location and orientation of the failure modes observed during manufacturing. A quantitative evaluation of the ability of the analysis to predict the stresses is hampered by the inability to measure the stresses directly. The model had to be judged on its ability to predict gross displacement behavior and structural fracture trends. Various elements of the model, such as boundary conditions, structural flexibility, and thermal and mechanical loading, were manipulated in search of an adequate predictive model. The work started with a single laminated cylindrical shell panel analyzed according to classical shell theory. The influence of the press platens during the manufacturing operation was introduced as imposed forces and displacement constraints. The fully rigid model produced unrealistic results and had to be discarded. The unrestrained model produced more realistic results and formed the basis for further refined studies.

The structural response for a composite panel without the constraints of the laminating press is substantially more complicated since the equilibrium shape or force distribution is unknown. The thermal-elastic behavior of a laminate plate out-of-the-press was solved using a Rayleigh-Ritz approximation technique. This model was useful in predicting only part of the observed behavior. A more sophisticated structural model including transverse shear was needed to explain fully all of the observed failure modes.

This paper describes the development of a thermal stress analysis capability based on the classical shell theory. The analysis is based on the assumption that heat flow occurs only in the radial direction, i.e., the heat transfer problem to be solved is one dimensional. Each layer of the ceramic may be isotropic, transversely isotropic, or orthotropic. If the material is orthotropic, the material axes must coincide with the structure axes, which are parallel to the sides of the rectangular panel. While a perfect bond is assumed between all layers, the layers are assumed to carry no load until the ceramic is below a preassigned freeze temperature. Results were obtained for a variety of boundary conditions, material properties, and load conditions.

Received Oct. 12, 1978; revision received Feb. 19, 1980.

*Associate Professor of Civil Engineering.
†Member, Technical Staff, TRW Defense and Space Systems Groups; formerly, Research Assistant, Case Western Reserve University.
‡Professor of Mechanical and Aerospace Engineering.

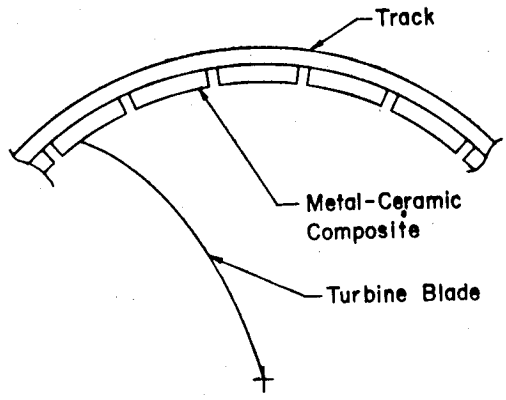

Fig. 1 Section of jet engine illustrating the use of abradable seals.

There is a substantial body of literature dealing with the analysis of composite plates and cylindrical shells. Solutions using a classical thin shell theory have been given by Reissner and Stavsky,[1] Dong et al.,[2] and Stavsky.[3] Most of these solutions deal with either a full cylinder or a panel supported on at least two edges. In this work, the case of free-edge boundary conditions is treated.

The paper presents an application of a well established theory for the prediction of the thermal structural response of metal-ceramic composites. Only the "freezing" aspects of the analysis represent a contribution to the theory. Confidence in the theory and the computer programs used to generate the results allowed the authors to make recommendations on the design of the laminates and the manufacturing procedures.

Similar problems in thermal structural analysis of layered composites occur in the deposition of thin film onto substraits, the columnar solidification of eutectics and alloys, or the systematic removal of material through grinding or machining.

Problem Description

The layered cylindrical shell panel to be analyzed is shown in Fig. 2. The analysis is based on classical thin shell theory, which involves the following assumptions: 1) the shell is thin; 2) the deflections of the shell are small compared to its thickness; 3) transverse normal stress is negligible; and 4) normals to the shell reference surface before deformation remain normal to it after deformation.[4]

Additional assumptions were made for the composite shell. Each layer is assumed to be homogeneous and elastic with thermal and mechanical properties which may be functions of temperature. Elastic properties may be isotropic, transversely isotropic, or orthotropic. If the properties are orthotropic, the material and structural axes must coincide. It is assumed that the layers are perfectly bonded, so that there cannot be any relative movement between adjacent layers.

For all cases to be analyzed here, the edges of the panel are assumed to be free; displacements on the edge are unrestricted and the normal and shear stresses must be zero at all points in the edge. Three cases of conditions on the upper and lower surfaces have been considered:

Case I. All displacements suppressed—this condition corresponds to a panel confined between rigid platens of a press with full friction between panel and platens.

Case II. Changes in curvature are prevented, but in-plane displacement is possible—this condition corresponds to a panel confined between rigid platens with no friction between platens and panel.

Case III. No restraints on displacements anywhere in the shell. This is the case of a completely free panel cooling in an unrestrained manner after removal from the press.

It should be noted that because transverse shear deformations and normal stresses are neglected, the classical theory cannot distinguish between top and bottom surface boundary conditions, which means they must be the same in the analysis.[5]

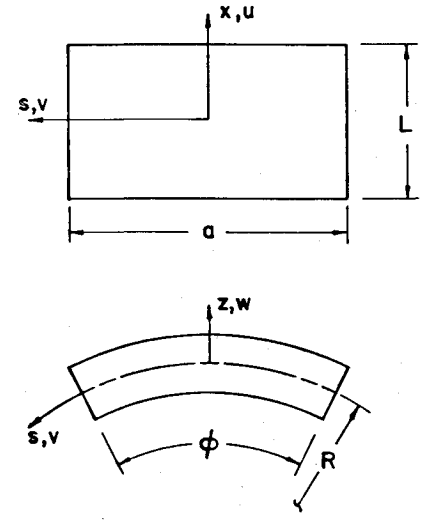

Fig. 2 Cylindrical shell.

Force Strain Relations

The first step in the analysis is to develop a set of force-strain equations relating resulting forces per unit width to reference surface strains and curvatures. The stress-strain relation for an arbitrary point in a layer i can be written in matrix form as

$$\begin{bmatrix}\sigma_{11}\\ \sigma_{22}\\ \sigma_{12}\end{bmatrix}^i = \begin{bmatrix}\frac{E_{11}}{1-\nu_{21}\nu_{12}} & \frac{E_{11}\nu_{12}}{1-\nu_{21}\nu_{12}} & 0\\ \frac{E_{22}\nu_{21}}{1-\nu_{21}\nu_{12}} & \frac{E_{22}}{1-\nu_{21}\nu_{12}} & 0\\ 0 & 0 & G_{12}\end{bmatrix}^i \begin{bmatrix}\epsilon^T_{11}\\ \epsilon^T_{22}\\ \epsilon^T_{12}\end{bmatrix}$$

$$- \begin{bmatrix}\frac{E_{11}}{1-\nu_{12}\nu_{21}} & \frac{E_{11}\nu_{12}}{1-\nu_{12}\nu_{21}} & 0\\ \frac{E_{22}\nu_{21}}{1-\nu_{12}\nu_{21}} & \frac{E_{22}}{1-\nu_{12}\nu_{21}} & 0\\ 0 & 0 & G_{12}\end{bmatrix}^i \begin{bmatrix}\alpha_{11}\Delta T\\ \alpha_{22}\Delta T\\ 0\end{bmatrix}^i \tag{1a}$$

or

$$\begin{bmatrix}\sigma_{11}\\ \sigma_{22}\\ \sigma_{12}\end{bmatrix}^i = \begin{bmatrix}Q_{11} & Q_{12} & 0\\ Q_{12} & Q_{22} & 0\\ 0 & 0 & Q_{33}\end{bmatrix}^i \begin{bmatrix}\epsilon^T_{11}\\ \epsilon^T_{22}\\ \epsilon^T_{12}\end{bmatrix}$$

$$- \begin{bmatrix}Q_{11} & Q_{12} & 0\\ Q_{12} & Q_{22} & 0\\ 0 & 0 & Q_{33}\end{bmatrix}^i \begin{bmatrix}\alpha_{11}\Delta T\\ \alpha_{22}\Delta T\\ 0\end{bmatrix}^i \tag{1b}$$

There will be an expression of this type for each of the layers in the composite shell. In these expressions, the superscript T indicates total strain and $E_{11}\nu_{12}=E_{22}\nu_{21}$. The term ΔT is the temperature change that the laminate experiences between the fabrication temperature and the inspection temperature. Initially the fabrication temperatures are taken to be the stress-free temperatures observed at the equilibrium conditions of a uniform gradient between the outside ceramic

layer and the metallic layer. These temperatures are shown in Table 1.

The displacements at any point through the thickness can be written

$$u^T = u - zw_{,x}; v^T = v - z\left\{\frac{-v}{R} + w_{,s}\right\}; w_{,z} = 0 \tag{2}$$

$$\epsilon_x^T = u_{,x} - zw_{,xx} = \epsilon_x + z\kappa_x$$

$$\epsilon_s^T = v_{,s} + \frac{w}{R} + z\left\{\frac{v_{,s}}{R} - w_{,ss}\right\} = \epsilon_s + z\kappa_s$$

$$\epsilon_{sx}^T = u_{,s} + v_{,x} + z\left\{\frac{v_{,x}}{R} - 2w_{,xs}\right\} = \epsilon_{sx} + z\kappa_{sx} \tag{3}$$

where u,v are reference surface displacements. Substituting these results into Eq. (1) leads to

$$\{\sigma\}^i = [Q]^i\{\epsilon\} + z[Q]^i\{\kappa\} - [Q]^i\{\alpha\Delta T\}^i \tag{4}$$

The temperatures are assumed to vary linearly within a given layer, so ΔT in Eq. (4) can be written $\Delta T = T_0 + zT_1$.

The stress-strain relations can now be integrated through the thickness to obtain a set of force-strain relations. Define the forces and moments to be

$N = \int \sigma dz$ = resultant force/unit width

$M = \int z\sigma dz$ = resultant moment/unit width about the reference surface

Consider as an example N_x, the membrane force/unit width in the x direction,

$$N_x = \int \sigma_x dz = \int \{Q_{11}\epsilon_x + Q_{12}\epsilon_s + zQ_{11}\kappa_x + zQ_{12}\kappa_s - Q_{11}\alpha_x\Delta T - Q_{12}\alpha_s\Delta T\}dz$$

Since the properties change from layer to layer, but are constant within one layer, the integration must be carried out in a piecewise fashion. With the plies numbered from one to n from bottom to top:

$$N_x = \int\Big\{\sum_{i=1}^{n} Q_{11}^i\epsilon_x + \sum_{i=1}^{n} Q_{12}^i\epsilon_s + \sum_{i=1}^{n} Q_{11}^i z\kappa_x + \sum_{i=1}^{n} Q_{12}^i z\kappa_s - \sum_{i=1}^{n} Q_{11}^i\alpha_x^i(T_0 + T_1 z)^i - \sum_{i=1}^{n} Q_{12}^i\alpha_s^i(T_0 + T_1 z)^i\Big\}dz$$

Interchanging the summation and integration, and carrying out the integration gives

$$N_x = \epsilon_x \sum_{i=1}^{n} Q_{11}^i(h_{i+1} - h_i) + \epsilon_s \sum_{i=1}^{n} Q_{12}^i(h_{i+1} - h_i) + \kappa_x \sum_{i=1}^{n} Q_{11}^i\left\{\frac{h_{i+1}^2 - h_i^2}{2}\right\} + \kappa_s \sum_{i=1}^{n} Q_{12}^i\left\{\frac{h_{i+1}^2 - h_i^2}{2}\right\} - \sum_{i=1}^{n} Q_{11}^i\alpha_x^i\left\{T_0(h_{i+1} - h_i) + T_1\frac{h_{i+1}^2 - h_i^2}{2}\right\}^i - \sum_{i=1}^{n} Q_{12}^i\alpha_s^i\left\{T_0(h_{i+1} - h_i) + T_1\frac{h_{i+1}^2 - h_i^2}{2}\right\}^i$$

or

$$N_x = A_{11}\epsilon_x + A_{12}\epsilon_s + B_{11}\kappa_x + B_{12}\kappa_s - \bar{N}_x$$

Table 1 Stress-free temperature and temperatures at time of analysis of metal-ceramic composite

Layer	Stress-free temperatures, °F[a] Top	Bottom	Temperature at time of analysis, °F Top	Bottom
1	5000.0	4199.0	1357.2	1133.5
2	4199.0	3929.0	1133.5	1080.3
3	3929.0	3617.0	1080.3	1029.5
4	3617.0	3267.0	1029.5	980.2
5	3267.0	2891.0	980.2	931.9
Substrate	2891.0	2700.0	931.9	899.7

[a] 1°C = 1.8°F.

Following the same procedure for all of the resultant forces and moments, the resulting force-strain relations can be written

$$\begin{bmatrix} N_x \\ N_s \\ N_{sx} \\ \hline M_x \\ M_s \\ M_{xs} \end{bmatrix} = \left[\begin{array}{ccc|ccc} A_{11} & A_{12} & 0 & B_{11} & B_{12} & 0 \\ A_{12} & A_{22} & 0 & B_{12} & B_{22} & 0 \\ 0 & 0 & A_{33} & 0 & 0 & B_{33} \\ \hline B_{11} & B_{12} & 0 & D_{11} & D_{12} & 0 \\ B_{12} & B_{22} & 0 & D_{12} & D_{22} & 0 \\ 0 & 0 & B_{33} & 0 & 0 & D_{33} \end{array}\right] \times \left[\begin{array}{c} \epsilon_x \\ \epsilon_s \\ \epsilon_{sx} \\ \hline \kappa_x \\ \kappa_s \\ \kappa_{sx} \end{array}\right] - \left[\begin{array}{c} \bar{N}_x \\ \bar{N}_s \\ 0 \\ \hline \bar{M}_x \\ \bar{M}_s \\ 0 \end{array}\right] \tag{5}$$

The details of the derivations and expressions for the A's, B's, C's and D's can be found in Ref. 3. $\bar{N}_x, \bar{N}_s$ are the resultant thermal thrusts while $\bar{M}_x$ and $\bar{M}_s$ are the resultant thermal moments, and their derivation can be found in Ref. 6.

Solutions Directly from the Force-Strain Relations

Solutions to problems with certain conditions can be obtained directly from the force-strain relations. For case I, full friction between the panel and press, all changes in geometry except possibly a uniform transverse displacement are prevented. The imposed displacements to achieve this constraint can be expressed in terms of the following strain and curvature conditions.

$$\epsilon_x = \epsilon_{sx} = 0$$

$$\kappa_x = \kappa_s = \kappa_{sx} = 0$$

$$\epsilon_s = w_s/R$$

for every point in the planform. Here w_s is the uniform displacement imposed on the panel by the platens. Referring to Eq. (5), it can be seen that since the thermal thrusts and moments are known quantities and the strains are known, the resultant forces and moments can be calculated directly. The stresses can be calculated directly using the stress-strain relations, Eq. (1a).

The composite panel shown in Fig. 3 was analyzed for the temperature distribution shown in Table 1. Also shown in

Table 2 Table of coefficients for structural properties as a function of temperature for metal-ceramic composite
Property $= A + BT + CT^2$

Coefficient	Layer 1	Layer 2	Layer 3	Layer 4	Layer 5	Substrate
Young's modulus, psi[a]						
A	363,000	3,130,000	4,050,000	3,220,000	5,250,000	32,670,000
B	—	—	—	—	—	−3609
C	—	—	—	—	—	0.8715
Coefficient of thermal expansion, F°[b]						
$A \times 10^5$	0.5164	0.2448	0.3728	0.6134	0.8468	0.5691
$B \times 10^8$	0.0436	0.3652	0.2342	0.2732	0.1437	0.4254
Poisson's ratio						
	0.25	0.26	0.28	0.29	0.31	0.32

[a] 1 psi = 6.9 kN/m^2. [b] 1°C = 1.8°F.

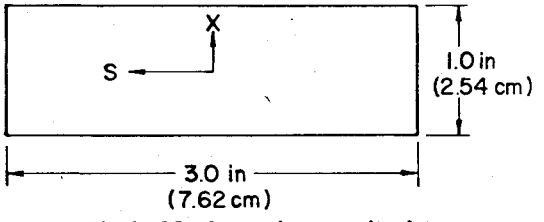

Fig. 3 Metal-ceramic composite plate.

Table 1 is the assumed stress-free temperature distribution. These temperature distributions are obtained from a one-dimensional heat transfer analysis. The composite is assumed to be made of materials with temperature-dependent thermal properties. The one-dimensional nature of the analysis assumes all heat transfer to take place in the through thickness direction. This ignores the heat lost through the edges of the composite and so represents an approximation. The elastic properties are assumed to be isotropic and parabolic functions of temperature. The properties assumed for the example problems to be discussed are shown in Table 2. These are the properties for typical ceramic and metal-ceramic materials as well as for the substrate, which is metallic.

The results of this analysis are shown in Fig. 4. This plot shows the x direction normal stress, which is the same at all points in the planform. It can be seen that almost all of the load required to maintain the undeformed shape is resisted by the substrate. The magnitudes of the stresses are much higher than the materials could reasonably be expected to resist. The full friction model is evidently not a realistic one for this particular structure. This model requires an extremely high frictional force between the metallic layer and the platen surface and a correspondingly high interlaminar shear stress between the metallic layer and the ceramic layers to develop the high normal stresses. Even if these forces were available, the metallic substrate and the ceramic layers would not sustain the loads. The metallic layer would yield, the interface would debond, and the ceramic would fail. In fact a ceramic layer will not sustain a significant load level until the temperature drops below a certain level defined as the freeze temperature. Below this temperature the layer is assumed to be fully effective. Realistically the structural change at the freeze point is a gradual transition. Nevertheless the approximation of a freeze temperature analysis is a reasonable estimate of the solidification process. Using a uniform freeze temperature of 1800°F (982°C) as the fabrication temperature and assuming that the structure solidifies from the metallic layer outward the analysis is repeated. A substantial change in the results is observed, namely the stress magnitudes are reduced. The results are shown as the second graph in Fig. 4. In spite of this change, the results remain unrealistically high. Therefore case I, full friction constrain during fabrication, is discarded as an unrealistic approximation.

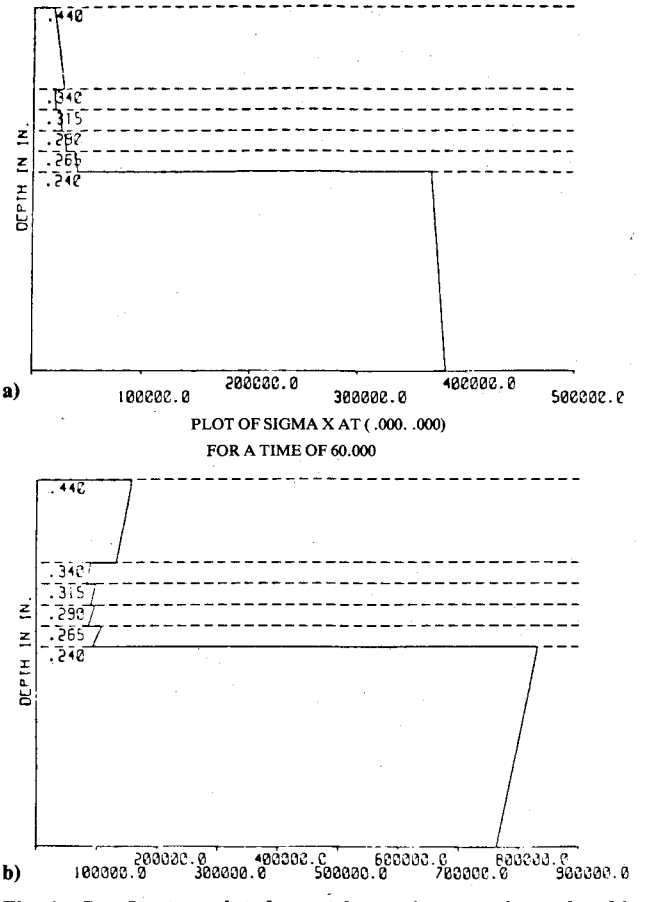

Fig. 4 Case I—stress plots for metal-ceramic composite analyzed in the press under full friction conditions using classical shell theory. a) Freeze temperature analysis; b) solid, stress-free analysis.

Case II, which can also be solved directly using the force-strain relations, as the in-press, no friction case in which the panel is confined between rigid platens, but it is assumed that there is no restraint to tangential motion provided by the platens. For this case, the changes in curvature must be zero and the in-plane forces must be zero.

$$N_x = N_s = N_{sx} = 0$$

$$\kappa_x = \kappa_s = \kappa_{sx} = 0$$

Referring to Eq. (5), it can be seen that the strains can be obtained directly as

$$\epsilon_x = \frac{A_{22}p_1 - A_{12}p_2}{A_{11}A_{22} - A_{12}^2}$$

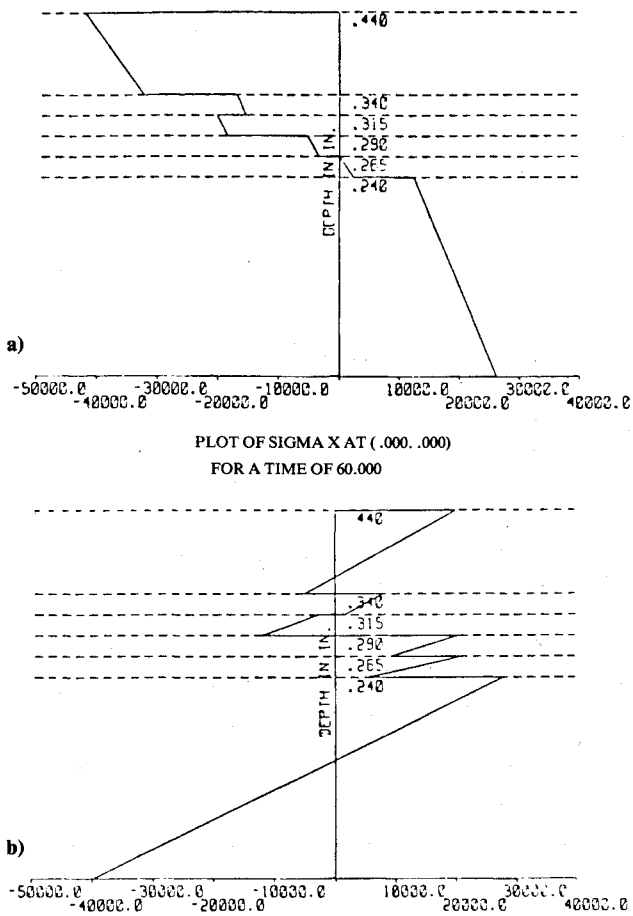

Fig. 5 Case II—stress plots for metal-ceramic composite analyzed in the press under friction-free conditions using classical shell theory. a) Freeze temperature analysis; b) solid, stress-free analysis.

$$\epsilon_s = \frac{A_{11}p_2 - A_{12}p_1}{A_{11}A_{22} - A_{12}^2}$$

$$\epsilon_{sx} = 0$$

in which

$$p_1 = \bar{N}_x - A_{12}(w_s/R), \quad p_2 = \bar{N}_s - (A_{22}w_s/R)$$

With the strains calculated, the resultant moments can be calculated directly from the lower part of Eq. (5).

The same panel analyzed in the previous example was analyzed for the friction-free boundary conditions. A plot of the x direction normal stresses is shown in Fig. 5. The stresses in this case are much smaller than those from the full friction case and the distribution is entirely different. In the present case, the stresses are required to prevent any change in curvature of the panel. There is relatively little tendency for the composite to bend for the combination of thermal and mechanical properties used in this example; thus the stresses generated are much smaller than those required to prevent all tangential displacement. The results do indicate an explanation of one of the observed failure mechanisms. The large normal stress discontinuity between the metallic and ceramic layers as well as several of the lamina of the ceramic suggest a delamination failure. However, the classical shell analysis does not include the effects of transverse shear deformation and the interlaminal shear stresses are indeterminant. Therefore, the normal stress discontinuities only suggest the possibility of high interlaminar shear stresses, and a more sophisticated model including transverse shear deformations would be required to give satisfactory estimates of the shear stress magnitudes.

The stress patterns shown in Fig. 5 for the solid stress-free analysis indicate a residual compressive stress in the outside of the metallic layer and a residual tensile stress in the outside of the ceramic layer. Since these stresses exist in the laminate while it is held in the press, the laminate will deform into a new equilibrium shape upon removal from the press. The laminate will bend with the metallic layer on the outside and the ceramic layer on the inside of the curve. This deformed equilibrium shape is consistent with experimentally observed results.

The calculations were repeated using a uniform freeze temperature of 1800°F (982°C) in the ceramic layers. The magnitudes of the stresses are essentially unchanged; however, the character of the stress pattern is different.

The stress pattern for the freeze temperature analysis exhibits a reversal of stresses, so that upon removal from the press the laminate will deform in the opposite direction, with the ceramic on the outside of the curve. This deformed shape was not observed experimentally.

The stress results for this case are independent of location in the planform. The delamination or tensile stresses in the ceramic are uniform over the span. Since the delamination stresses occur near the edges and the tensile stresses occur near the center this model seemed inadequate for predicting the failure mechanisms.

The friction free analysis (case II) can be used to obtain an alternative full friction analysis (case I) which is more realistic than the one previously described. In the case I full friction analysis, the platens were assumed to be completely rigid, with no thermal expansion allowed. Although the platens are certainly more rigid than the metal-ceramic composite panel, they will expand and contract as their temperature changes. An analysis that includes the thermal expansion and contraction of the platens while at the same time preventing relative motion between the platens and the composite can be carried out by including the platens as additional layers in a friction-free analysis. Results for this proposed model are not presented, but indicate a reduction of the extremely large stress magnitudes observed in the rigid platen analysis.

Case III for a cooling out of the press can be separated into two subcases, the flat panel and the curved panel.

A solution can be obtained directly from the force-strain relations of a flat composite with no external restraints subject to a temperature change. In the unrestrained case for a curved panel, the strains obtained from the force-strain relations do not lead to displacement fields which satisfy the boundary conditions and the strain-displacement relations. Thus, an approximate solution using the Rayleigh-Ritz technique must be used for the curved panel.

For the flat plate without external restraints subjected to an arbitrary temperature change through the thickness, the resultant forces and moments of any section must be zero, since there are no external loads or reactions. Since there is no variation in the planform for this theory, it can be said that

$$N_x = N_s = N_{xs} = 0, \quad M_x = M_s = M_{xs} = 0$$

everywhere in the planform. Referring to Eq. (5), it can be seen that the reference surface strains and the curvatures can be obtained directly. Using these strains and the displacement boundary conditions in the strain-displacement relations, the displacements can be obtained by integration. The displacement boundary conditions are

$$\text{at} \quad x = s = 0; \quad w = 0$$

$$\text{along} \quad x = 0 \quad u = 0, \quad w_{,x} = 0$$

$$\text{along} \quad s = 0 \quad v = 0, \quad w_{,s} = 0$$

The resulting displacement field, which satisfies the boundary conditions and leads to stresses which satisfy

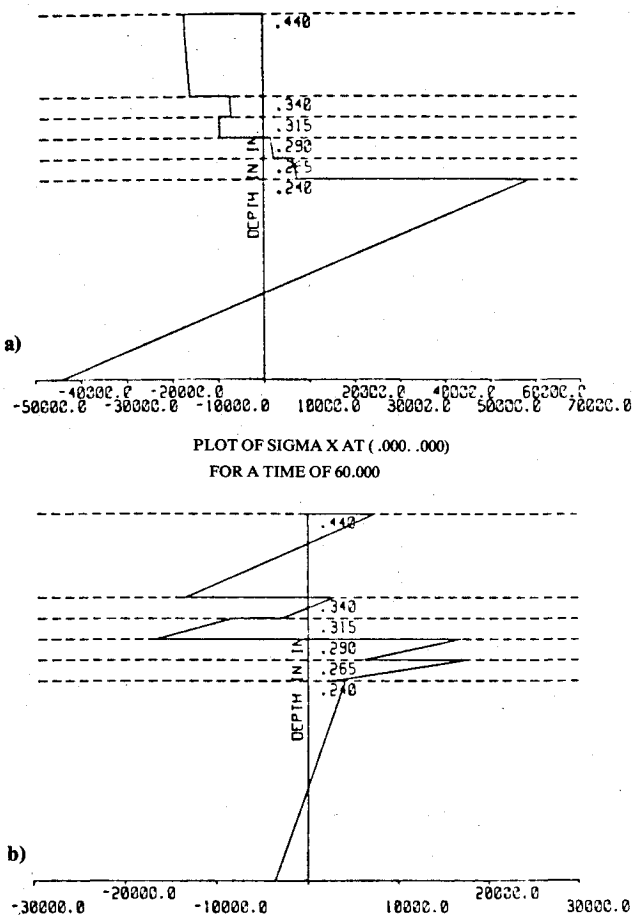

Fig. 6 Case III (flat plate)—stress plots for flat metal-ceramic composite plate analyzed out of the press using classical shell theory. a) Freeze temperature analysis; b) solid, stress-free analysis.

equilibrium, is

$$u=\epsilon_x^x, \quad v=\epsilon_s^s, \quad w=-\tfrac{1}{2}(\kappa_x x^2+\kappa_s s^2)$$

Within the limitations of classical composite plate theory, these displacements represent the exact solution for a free composite plate subjected to an arbitrary temperature change through the thickness.

The composite plate used previously was analyzed for the out-of-press conditions using the same temperature changes used previously. The results are shown in Fig. 6. As in the other cases, the stresses predicted in the ceramic are rather high. This model also predicts strains and curvatures which are uniform over the planform. The stress predictions for the solid stress free analysis suggests two possible ceramic layer and delamination between ceramic layers.

The analysis was repeated for a freeze temperature analysis of 1800°F (982°C). The stress patterns observed for this model are consistent with the experimental results of compression in the outside ceramic layer and high interlaminate stresses at the metal/ceramic interface.

Both thermal load conditions produced deformed shapes with the ceramic on the inside of the curve. This deformed shape is consistent with the experimentally observed results.

This flat plate model represents the most promising results in correlating qualitatively with the observed experimental results. Two factors remain to be considered. The model does not include the effects of initial curvature or the effects of transverse shear deformation. Within the theory formulated and presented herein, the effects of curvature can be evaluated. A more sophisticated theory is needed to treat transverse shear deformations.

Energy Formulation

For the case of the curved panel cooling in an unrestrained manner, a solution cannot be obtained from the force-strain relation directly. In this work, the Rayleigh-Ritz technique[7] was employed to achieve a solution. A set of assumed displacement functions satisfying the kinematic boundary conditions containing unknown coefficients is substituted in the total potential energy expression for the shell and the unknown coefficients chosen so as to minimize the total potential energy. The total potential energy expression can be written in terms of resultant forces and strains as

$$\pi_p=\frac{1}{2}\iint_S \{N_x\epsilon_x+M_x\kappa_x+N_s\epsilon_s+M_s\kappa_s+N_{sx}\epsilon_{sx}+M_{sx}\kappa_{sx} -2\bar{N}_x\epsilon_x-2\bar{M}_x\kappa_x-2N_s\epsilon_s-2M_s\kappa_s\}\,dS \tag{6}$$

where S indicates that the integration is carried out over the reference surface. Utilizing the strain-displacement relations [Eq. (2)] and the force-strain relations [Eq. (1)], π_p can be written in terms of displacements as

$$\begin{aligned}\pi_p=\frac{1}{2}\iint_S \Big\{&A_{11}u_{,x}^2+\left[A_{33}+\frac{2B_{33}}{R}+\frac{D_{33}}{R^2}\right]v_{,x}^2\\&+\left[A_{22}+\frac{2B_{22}}{R}+\frac{D_{22}}{R^2}\right]v_{,s}^2+2\left[A_{12}+\frac{B_{12}}{R}\right]u_{,x}v_{,s}\\&+2\left[A_{33}+\frac{B_{33}}{R}\right]u_{,s}v_{,x}+A_{33}u_{,s}^2+\frac{2A_{12}}{R}u_{,x}w-2B_{11}u_{,x}w_{,xx}\\&-2B_{12}u_{,x}w_{,ss}-4B_{33}u_{,s}w_{,sx}-4\left[B_{33}+\frac{D_{33}}{R}\right]v_{,x}w_{,xs}\\&+\frac{2}{R}\left[A_{22}+\frac{B_{22}}{R}\right]v_{,s}w-2\left[B_{12}+\frac{D_{12}}{R}\right]v_{,s}w_{,xx}\\&-2\left[B_{22}+\frac{D_{22}}{R}\right]v_{,s}w_{,ss}+\frac{A_{22}}{R^2}w^2-\frac{2B_{22}}{R}w_{,ss}w\\&-\frac{2B_{12}}{R}ww_{,xx}+D_{11}w_{,xx}^2+D_{22}w_{,ss}^2+4D_{33}w_{,sx}^2+2D_{12}w_{,xx}w_{,ss}\\&-2\bar{N}_xu_{,x}-2\left[\bar{N}_s+\frac{\bar{M}_s}{R}\right]v_{,x}-\frac{2\bar{N}_s}{R}w+2\bar{M}_xw_{,xx}+2\bar{M}_sw_{,ss}\Big\}\,dS\end{aligned} \tag{7}$$

The assumed displacement functions must be continuous, satisfy the kinematic boundary conditions given earlier, and be capable of representing the deflected shape of the shell reasonably well. The displacement functions used in this work are

$$\begin{aligned}w&=\sum_{n=0}^{\infty}\sum_{m=0}^{\infty}a_{mn}\cos\frac{n\pi x}{\ell}\cos\frac{m\pi s}{a}\\u&=\alpha x+\sum_{n=0}^{\infty}\sum_{m=0}^{\infty}b_{mn}\sin\frac{n\pi x}{\ell}\cos\frac{m\pi s}{s}\\v&=\beta s+\sum_{n=0}^{\infty}\sum_{m=0}^{\infty}c_{mn}\cos\frac{n\pi x}{\ell}\sin\frac{m\pi s}{a}\end{aligned} \tag{8}$$

in the interval

$$-\ell/2\le x\le\ell/2, \quad -a/2\le s\le a/2$$

where a and ℓ are the planform dimensions of the shell, a_{mn}, b_{mn}, and c_{mn} are unknown coefficients to be determined so as

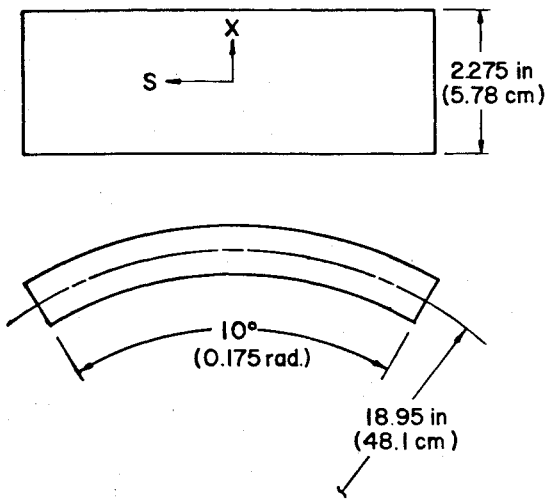

Fig. 7 Schematic of cylindrical metal-ceramic composite shell.

to render π_p a minimum. The terms αx in the expression for u and βs in the expression for v represent free expansion of a plate and are added to the solution to speed convergence.

By using the force equilibrium equations, it is possible to express b_{mn} and c_{mn} in terms of a_{mn} so that the minimization of the total potential energy can be carried out only with respect to a_{mn}. Thus, for given values of m and n, the number of unknown coefficients to be solved for is cut by a factor of three. The expressions for b_{mn} and c_{mn} in terms of a_{mn} are

$$b_{mn} = X_{mn} a_{mn}, \quad c_{mn} = Y_{mn} a_{mn}$$

X_{mn} and Y_{mn} are constants for a given set of indices m and n and are functions of m, n, a, ℓ, and the elastic constants of the shell. Details of the derivation of X_{mn} and Y_{mn} are available in Appendix A of Ref. 6. The final form of the displacement functions is then

$$w = \sum_{n=0}^{\infty} \sum_{m=0}^{\infty} a_{mn} \cos \frac{n\pi x}{\ell} \cos \frac{m\pi s}{a}$$

$$u = \alpha x + \sum_{n=0}^{\infty} \sum_{m=0}^{\infty} X_{mn} a_{mn} \sin \frac{n\pi x}{\ell} \cos \frac{m\pi s}{a}$$

$$v = \beta s + \sum_{n=0}^{\infty} \sum_{m=0}^{\infty} Y_{mn} a_{mn} \cos \frac{n\pi x}{\ell} \sin \frac{m\pi s}{a}$$

These displacement functions are substituted into Eq. (7) for the total potential energy and integration over the planform carried out. The set of coefficients a_{mn} which minimize π_p is found by differentiating π_p and solving the resulting set of simultaneous equations. In contrast to the usual Rayleigh-Ritz analysis, the displacement functions used in this analysis are not orthogonal, so that the set of equations does not uncouple. The coefficient matrix of the set of simultaneous equations is fully populated and tends to become ill-conditioned as more and more modes are added.

The composite shell shown in Fig. 7 with the same material properties as the plate used in previous examples, was analyzed for out of press conditions. Figure 8 shows a plot of the x direction normal stress near the corner of the shell. In this analysis, the stresses vary over the planform. For the relatively shallow shell analyzed in this example, variation in normal stresses over the planform is less than 5% and the shear stresses are quite small. Comparing the plots of Fig. 8 with those of Fig. 6, it is clear that for the geometry of this example, a good approximation for these data can be

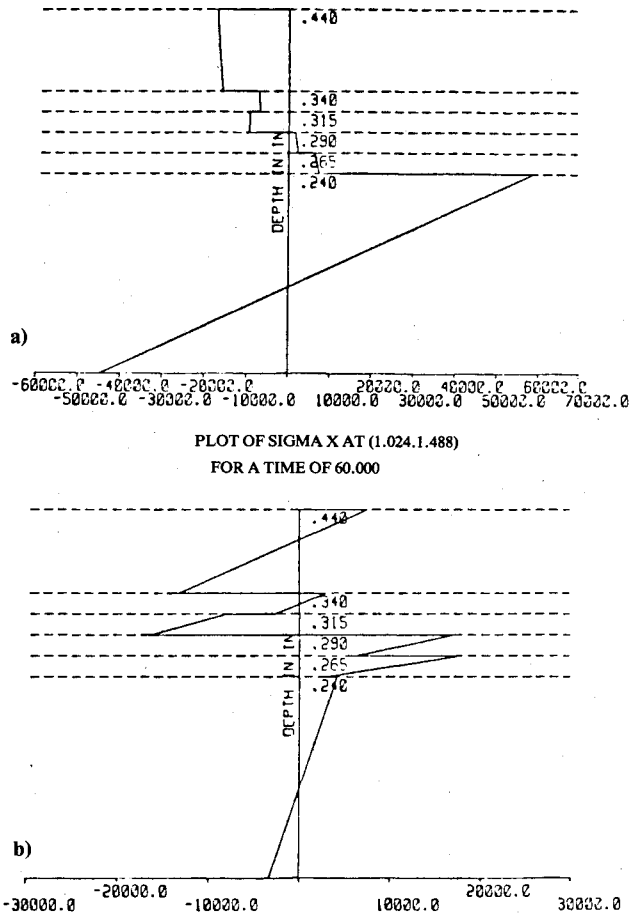

Fig. 8 Case III (curved panel)—typical stress plate for cylindrical metal-ceramic composite shell analyzed out of the press using classical shell theory. a) Freeze temperature analysis; b) solid, stress-free analysis.

achieved by ignoring the curvature. A substantial saving in computational effort can be realized by doing only a flat plate analysis. These observations can be made for both thermal analyses; the solid, stress force analysis and the freeze temperature analysis.

The case III model using either the flat plate or the curved panel and the freeze temperature thermal conditioning provides analytical results which provide the best correlation with the experimental results. The deformed shape for this case is consistent with experimental results. The discontinuity in the normal stress across the substrate/ceramic interface suggest the presence of a large interlaminar shear stress. Accurate predictions of these delaminating stresses requires an analysis which includes transverse shear deformation. Finally, the freeze temperature analysis for case III predicts a compressive stress on the outside of the ceramic layer. These observations lead to the conclusion that the case III model provides the superior model based on classical theory.

Conclusions

An analysis of a layered composite cylindrical shell panel based on classical shell theory has been presented. For most of the cases of interest, the solution is obtained at very little computational effort directly from the force-strain relations. For one case, the solution must be obtained using a more costly Rayleigh-Ritz solution.

The analysis presented gives an idea of the gross stress and deflection response of a layered composite cylindrical shell panel subjected to an arbitrary distribution of temperature through the thickness of the composite. The temperature is

assumed invariant with respect to planform location. The unconstrained cooling from a freeze temperature of the ceramic/metallic composite laminate provides the most realistic results. This model correlates with the gross deformation pattern as well as the location and character of stresses which will cause failure.

During production of this type of composite, delamination failures are frequently a problem. The analysis outlined here provides limited information to help avoid failures of this type. To obtain accurate interlaminar shear stress prediction which cause delamination to occur, it is necessary to include the effect of transverse shear deformations in the analysis.

Acknowledgment

The research described here was supported by the Parma Technical Center of the Union Carbide Corporation. Their financial support, cooperation and advice throughout the work are gratefully acknowledged. Particular thanks are due to Dr. Roger Bacon, Dr. George Spence, Dr. Ray Sara and Dr. Robert Schepler, all of the Parma Technical Center.

References

[1] Reissner, E. and Stavsky, Y., "Bending and Stretching of Certain Types of Heterogeneous Aeolotropic Elastic Plates," *Journal of Applied Mechanics*, Vol. 28, Sept. 1961, pp. 403-408.

[2] Dong, S. B., Pister, K., and Taylor, R. L., "On the Theory of Laminated Anisotropic Shells and Plates," *Journal of the Aerospace Sciences*, Vol. 29, Aug. 1962, pp. 969-975.

[3] Stavsky, Y., "Bending and Stretching of Laminated Aeolotropic Plates," *Journal of the Engineering Mechanics Division, ASCE*, Vol. 87, Dec. 1961, pp. 31-56.

[4] Ambartsumyan, S. A., *Theory of Anisotropic Plates*, translated from Russian by T. Cheron, edited by J. E. Ashton, Technomic Publishing Co., Inc., Stamford, Conn., 1970.

[5] Whitney, J. M., "The Effect of Transverse Shear Deformation on the Bending of Laminated Plates," *Journal of Composite Materials*, Vol. 3, July 1969, pp. 534-547.

[6] Millavec, W. A., "Thermal Stress Analysis of Composite Shells," M.S. Thesis, Case Western Reserve University, 1977.

[7] Washizu, K., *Variational Methods in Elasticity and Plasticity*, 2nd Ed., Pergamon Press, Oxford, 1974.

[8] Miller, C. J., Millavec, W. A., and Kicher, T. P., "Thermal Stress Analysis of Layered Cylindrical Shells Including Transverse Shear Effects," submitted to *AIAA Journal*.